JOURNAL OF VIROLOGY, July 2004, p. 7352–7359 Vol. 78, No. 14
0022-538X/04/$08.00+0 DOI: 10.1128/JVI.78.14.7352–7359.2004

Sensitivity of NS3 Serine Proteases from Hepatitis C Virus Genotypes 2 and 3 to the Inhibitor BILN 2061

Diane Thibeault,* Christiane Bousquet, Rock Gingras, Lisette Lagacé, Roger Maurice, Peter W. White, and Daniel Lamarre†

Department of Biological Sciences, Boehringer Ingelheim (Canada) Ltd., Research and Development, Laval, Québec H7S 2G5, Canada

Received 3 February 2004/Accepted 12 March 2004

Hepatitis C virus (HCV) displays a high degree of genetic variability. Six genotypes and more than 50 subtypes have been identified to date. In this report, kinetic profiles were determined for NS3 proteases of genotypes 1a, 1b, 2ac, 2b, and 3a, revealing no major differences in activity. In vitro sensitivity studies with BILN 2061 showed a decrease in affinity for proteases of genotypes 2 and 3 (K_i, 80 to 90 nM) compared to genotype 1 enzymes (K_i, 1.5 nM). To understand the reduced sensitivity of genotypes 2 and 3 to BILN 2061, active-site residues in the proximity of the inhibitor binding site were replaced in the genotype-1b enzyme with the corresponding genotype-2b or -3a residues. The replacement of five residues at positions 78, 79, 80, 122, and 132 accounted for most of the reduced sensitivity of genotype 2b, while replacement of residue 168 alone could account for the reduced sensitivity of genotype 3a. BILN 2061 remains a potent inhibitor of these non-genotype-1 NS3–NS4A proteins, with K_i values below 100 nM. This in vitro potency, in conjunction with the good pharmacokinetic data reported for humans, suggests that there is potential for BILN 2061 as an antiviral agent for individuals infected with non-genotype-1 HCV.

According to the latest World Health Organization estimates, more than 170 million individuals may be infected with hepatitis C virus (HCV). Chronic infection, observed in about 85% of cases, could lead to progressive hepatic fibrosis, cirrhosis, and hepatocellular carcinoma (7). HCV belongs to the *Flaviviridae* family. Its positive-strand RNA genome contains 9,600 nucleotides and encodes a ~3,100-amino-acid protein that is posttranslationally processed by host- and virally encoded proteases into structural (C, E1, E2, p7) and nonstructural (NS2, NS3, NS4A, NS4B, NS5A, and NS5B) proteins (23). The nonstructural (NS) proteins include enzymes necessary for protein maturation (NS2/3 and NS3 proteases) and viral replication (NS3 helicase/nucleoside triphosphatase and NS5B RNA polymerase).

The high rate of viral production linked to the low fidelity of the RNA polymerases (5, 6) leads to genetic heterogeneity of HCV in infected patients (20). Natural variants of HCV are currently classified into 6 genotypes and more than 50 subtypes (25). The genotypes differ by as much as 34% in their nucleotide sequences, resulting in approximately 30% amino acid sequence divergence between the encoded polyproteins, while subtypes can differ by as much as 23% of their nucleotide sequence. The degree of sequence variability also varies for the different subgenomic regions. For example, the core and the 3′ and 5′ nontranslated regions are more conserved, whereas the envelope region displays more variability (24, 31). Sequences coding for the NS3 protease domain and the NS5B polymerase show degrees of variability comparable to that for the complete genome.

The HCV infections most frequently encountered are caused by genotypes 1, 2, and 3 (18). In Europe, Japan, and the United States, more than 70% of the HCV-positive population is infected with genotype 1 (18, 31). The spread of genotype 1b is slowing in Western countries, and genotypes 1a and 3a, mainly transmitted by infected intravenous drug users, constitute the main source of new infections (22, 31). No significant differences in the severity of illness are associated with the HCV genotype (7). However, the genotype is the major determinant of the outcome of therapy. Indeed, many HCV genotype-1 patients are refractory to interferon-based therapy, and only about 50% of patients treated with pegylated interferon and ribavirin for 48 weeks achieve a sustained virological response. On the other hand, about 80% of patients infected with HCV genotypes 2 and 3 achieve a sustained virological response with this treatment (4).

The higher prevalence and lower rate of response to treatment associated with HCV genotype 1 infections prompted us to focus our drug discovery efforts primarily on enzymes from this genotype. We targeted the serine protease activity responsible for viral maturation (26), which has been shown to be essential for HCV replication in vivo (11). Inhibitors of the HCV serine protease were designed through a substrate-based approach (15–17) which led to the discovery of the macrocyclic tripeptide inhibitor BILN 2061 (12). BILN 2061 is a potent and competitive inhibitor of the NS3 proteases of genotypes 1a and 1b, with inhibition constant (K_i) values in the low nanomolar range. Its administration to genotype-1-infected patients for 2 days resulted in an impressive reduction in HCV RNA plasma levels and established the first proof of concept in humans for an HCV NS3 protease inhibitor [H. Hinrichsen. Y. Benhamou,

* Corresponding author. Mailing address: Department of Biological Sciences, Boehringer Ingelheim (Canada) Ltd., Research and Development, 2100 Cunard St., Laval, Québec H7S 2G5, Canada. Phone: (450) 682-4640. Fax: (450) 682-8434. E-mail: dthibeault@lav.boehringer-ingelheim.com.

† Present address: Département de Médecine, Université de Montréal and Centre de Recherche du CHUM, Montréal, Québec H2X 1P1, Canada.

M. Reiser, R. Sentjens, H. Wedemeyer, J. L. Calleja, X. Forns, J. Croenlein, G. Nehmiz, and G. Steinmann, abstract from the 53rd Ann. Meet. Am. Assoc. Study Liver Dis., 2002, Hepatology **36**(Suppl. 1)**:**297A, 2002].

In this study, different natural variants of HCV NS3 protease are evaluated with regard to their kinetic properties and their sensitivity to BILN 2061. The full-length heterodimeric NS3–NS4A proteins of genotypes 2 and 3 and their respective NS3 protease domains were expressed in *Escherichia coli*, purified, characterized, and compared to genotype-1 enzymes, which were used for inhibitor optimization leading to BILN 2061. Very similar values for the kinetic parameters K_m and k_{cat} were observed for the various NS3–NS4A enzymes, while the sensitivity of genotype-2 and -3 enzymes to BILN 2061 was reduced relative to that of genotype 1, although the K_i was still in the low nanomolar range ($\leq$100 nM). Finally, residues that are different in different genotypes and are located in close proximity to the inhibitor binding site were substituted in genotype 1, and the chimeric enzymes were evaluated for their sensitivity to BILN 2061. Our data provide some insights into residues playing a role in inhibitor binding and, more importantly, suggest the beneficial potential of therapy with BILN 2061 in HCV genotype-2 and -3-infected individuals.

MATERIALS AND METHODS

Genetic constructs. The previously described NS3–NS4A coding region of genotype 1b, with a 28-residue N-terminal sequence containing a hexahistidine tag and a tobacco etch virus protease cleavage site (21), was amplified by PCR and then subcloned into the pET11a bacterial expression vector (Novagen). For genotype-2 and -3 enzymes, HCV RNA was isolated from serum samples, obtained before BILN 2061 administration, of patients infected with HCV genotypes 2ac, 2b, and 3a. The HCV genotype was determined by the INNO-LiPA HCV II test kit (Innogenetics, Ghent, Belgium). Viral RNA was extracted from 140 μl of serum by using a QIAamp viral RNA purification kit (QIAGEN). Isolated RNA was reverse transcribed into cDNA by using Superscript II (Gibco BRL) with HCV-specific primers corresponding to sequences located 3′ to the NS4A gene. The antisense primers for the HCV RNA were 5′-CTGATGAAG TTCCACATGTGCTTCGCCCAGAA-3′ for genotype 2b, 5′-ATTGAGGGAA GGTCCCCTGCCA-3′ for genotype 2ac, and 5′-CACAAAGTTCCACATGTG CTGTTGCCAGAA-3′ for genotype 3a. The cDNAs were used as templates for PCR amplification of a fragment spanning the NS3 and NS4A genes. The NS3–NS4A fragment for genotypes 2 and 3 was amplified by using primers corresponding to the six N-terminal amino acids of NS3 and the seven C-terminal amino acids encoded by the NS4A gene, since these amino acid sequences are highly conserved between genotypes and subtypes. The following primers were used: for genotype 2ac, forward primer 5′-CTCTGATCACGCTCCCATTACT GCTTACTCCCAG-3′ and reverse primer 5′-CACCGCTCGAGTCAACATTC CTCCATCTCATCAAAAGCC-3′; for genotype 2b, forward primer 5′-CTCGG ATCCGGCTCCCATTACTGCTTAC-3′ and reverse primer 5′-GACGCGTCGG ACGCGGCCGCTCAGCACTCTTCCATTTCATCGAA-3′; for genotype 3a, forward primer 5′-CTCGGATCCGGCCCCGATCACAGCATACGCC-3′ and reverse primer 5′-CACCGCTCGAGTCAGCATTCTTCCATCTCATCATATTG TTG-3′. The primers included restriction sites (underlined sequences) for cloning into the expression vector and a TGA termination codon in the antisense primer. PCR products were purified by agarose gel electrophoresis and subcloned into the pET11a bacterial expression vector. DNA sequencing was performed by using the Big Dye-Terminator Cycle Sequencing kit (Applied Biosystems), and sequences were analyzed on the ABI Prism 3100 Genetic Analyzer (Applied Biosystems).

Amino acid substitutions were introduced into the NS3–NS4A coding region by using the QuikChange II site-directed mutagenesis kit (Stratagene) according to the manufacturer's instructions. NS3 protease domain (amino acids 1 to 180) coding regions were amplified by PCR from the corresponding NS3–NS4A cDNA, by using a primer coding for the sequence ASKKKK at the C terminus, and were ligated into the pET29b bacterial expression vector (Novagen).

Expression and purification of the NS3-NS4A proteins from bacteria. The NS3–NS4A proteins (amino acids 1 to 685) were expressed in *E. coli* BL21(DE3) pLysS or, for genotype 1a, in *E. coli* Rosetta(DE3) cells (Novagen). Bacteria were grown at 37°C in CircleGrow medium (Q-BIOgene) supplemented with 100 μg of ampicillin/ml and 34 μg of chloramphenicol/ml. At mid-log phase, the culture was cooled to 22°C, and protein expression was induced with 0.5 mM isopropyl-β-D-thiogalactoside for 4 h. Then cells were harvested by centrifugation, and the cell paste was frozen at −80°C. The cell paste was resuspended in 5 ml of lysis buffer (50 mM $NaPO_4$ [pH 7.5], 20% glycerol, 1 mM EDTA, 0.5% Triton X-100, 0.5 M NaCl) per g of cells. For the genotype-1a enzyme, the lysis buffer was 50 mM $NaPO_4$ (pH 7.5)–40% glycerol–1 mM EDTA–0.5% Triton X-100. The suspension obtained was processed in a Dounce homogenizer, supplemented with 20 mM $MgCl_2$ and 10 μg of DNase I/ml, and incubated for 30 min on ice. The suspension obtained from *E. coli* Rosetta(DE3) cells was homogenized by using a microfluidizer. Following a brief sonication, the extract was clarified by a 30-min centrifugation at 150,000 × *g*. The supernatant was diluted twofold in 50 mM $NaPO_4$ (pH 7.5)–0.5 M NaCl, and imidazole was added to a final concentration of 25 mM. Then the solution was applied to a Hi-Trap Ni^{2+}-chelating column (Amersham Biosciences). The NS3–NS4A proteins were eluted in 50 mM $NaPO_4$ (pH 7.5)–0.5 M NaCl–10% glycerol–0.1% NP-40–5 mM imidazole by using a 5 to 500 mM imidazole gradient. The enzyme-enriched fractions were pooled, diluted fourfold in 50 mM $NaPO_4$ (pH 7.5)–10% glycerol–0.05% *n*-dodecyl-β-D-maltoside, and applied to a poly(U)-Sepharose affinity column (Amersham Biosciences) previously equilibrated in 50 mM $NaPO_4$ (pH 7.0)–10% glycerol–0.2 M NaCl–0.05% *n*-dodecyl-β-D-maltoside–10 mM β-mercaptoethanol. The enzyme was eluted in the same buffer containing 2 M NaCl. All of the enzymes were estimated to be more than 80% pure as judged by sodium dodecyl sulfate-polyacrylamide gel electrophoresis. The purified enzymes were stored at −80°C. The final yield ranged from 60 to 600 μg per liter of culture; the highest yield was obtained for the genotype-2b protease.

Expression and purification of the NS3 protease domains from bacteria. The NS3 protease domains (amino acids 1 to 180) were expressed in *E. coli* BL21(DE3) (genotypes 2b and 3a) or BL21(DE3) pLysS (genotypes 1a, 1b, and 2ac) cells (Novagen). Bacteria were grown at 37°C in CircleGrow medium supplemented with 30 μg of kanamycin/ml and 34 μg of chloramphenicol/ml. At mid-log phase, the culture was cooled to 22°C, and zinc acetate was added to a final concentration of 50 μM. Protein expression was induced with 1 mM isopropyl-β-D-thiogalactoside. Three hours postinduction, cells were harvested by centrifugation, and the cell paste was frozen at −80°C. The cell paste was resuspended in 5 ml of lysis buffer (25 mM $NaPO_4$ [pH 7.5], 10% glycerol, 1 mM EDTA, 0.1% octyl-β-D-glucoside, 15 mM NaCl) per g of cells. For the NS3 protease of genotype 3a, the lysis buffer contained 25 mM $NaPO_4$ (pH 7.5), 40% glycerol, 1 mM EDTA, and 0.5% Triton X-100. The suspension obtained from *E. coli* BL21(DE3) pLysS cells was processed in a Dounce homogenizer, supplemented with 20 mM $MgCl_2$ and 10 μg of DNase I/ml, and incubated for 20 min on ice, while the suspension obtained from *E. coli* BL21(DE3) cells was homogenized by using a microfluidizer. Following a brief sonication, the extract was clarified by a 30-min centrifugation at 21,200 × *g*. Then the purification was performed essentially as described previously (13). Briefly, the protease domains were purified from the soluble fraction by using SP-Sepharose, heparin, and Superdex 75 columns (Amersham Biosciences). Minor changes included the elution from the heparin column using an increased NaCl concentration, up to 450 mM, and the use of a modified buffer for the Superdex 75 column (25 mM HEPES [pH 7.0], 300 mM NaCl, 5 mM dithiothreitol). All of the enzymes were estimated to be more than 95% pure as judged by sodium dodecyl sulfate-polyacrylamide gel electrophoresis. The final yield varied from 55 to 450 μg of protein per liter of culture. The highest yield was observed for the genotype-1a protease.

Peptide and inhibitor synthesis. The substrate peptides DDIVPC-SMSYTW-OH and biotin-DDIVPC-SMSYTW-OH, derived from the NS5A/5B cleavage sequence (8), and the NS4A-derived peptides KKGCVVIVG RVVLSGKK (genotype 1a) and KKGSVVIVGRIILSGRK (genotype 1b) were prepared by using standard solid-phase peptide synthesis metholodogy (3). Additional NS4A cofactor peptides were obtained from Multiple Peptide Systems (San Diego, Calif.): KKGCVATIGRIHINHHK (genotype 2ac), KKGCISIIG RLHLNDRK (genotype 2b), and KKGCVVIVGHIELGGKK (genotype 3a). N-terminal and C-terminal lysines were added to enhance solubility. Each NS4A peptide matches the sequence of the corresponding NS4A protein as obtained from infected patients (see above). Radiolabeled biotin-DDIVPC-SMSY[^{125}I]TW-OH was prepared from the dimer form of the unlabeled peptide to protect the cysteine residue from oxidation. Following the introduction of ^{125}I (3.7 GBq/ml; Amersham Biosciences) by using the Iodogen procedure (Pierce), a reduction step was performed to generate the monomer form. The radiolabeled peptide was purified by reverse-phase high-performance liquid chromatography on a C_{18} column by using a gradient of 20 to 60% acetonitrile in water. The internally quenched depsipeptide fluorogenic substrates anthranilyl-DDI

VPAbu[C(O)-O]AMY(3-NO_2)TW-OH and anthranilyl-D(d)EIVP-NVal[C(O)-O]AMY(3-NO_2)TW-OH, designed on the basis of the NS5A/5B cleavage site, and Ac-DED(EDANS)EE-Abu[C(O)-O]ASK(DABCYL)-NH_2, designed on the basis of the NS4A/4B cleavage site, were synthesized according to the method previously described (2, 27). The synthesis of the macrocyclic inhibitor BILN 2061 has been described previously (30), and further details will be published elsewhere.

***K_m* and *k_{cat}* determination.** Kinetic parameters for the NS3-NS4A protein, the NS3 protease–$NS4A_{peptide}$ complex, and the NS3 protease domain from various genotypes were determined by using the depsipeptide fluorogenic substrate anthranilyl-DDIVPAbu[C(O)-O]AMY(3-NO_2)TW-OH. The cleavage reaction was continuously monitored at 23°C on a BMG POLARstar Galaxy fluorometer, equipped with excitation and emission filters of 320 and 405 nm, respectively, in the presence of 0.1 to 12 μM substrate. The NS3–NS4A protein (0.5 to 3 nM) was assayed in 50 mM Tris-HCl (pH 8.0)–0.25 M sodium citrate–0.01% *n*-dodecyl-β-D-maltoside–1 mM TCEP. The NS3 protease (5 to 50 nM) was assayed in 50 mM Tris-HCl (pH 7.5)–30% glycerol–1 mg of bovine serum albumin/ml–1 mM TCEP with or without a 1,000-fold molar excess of the $NS4A_{peptide}$. A 15-min preincubation was introduced to allow for the formation of the protease-NS4A peptide complex. Kinetic parameters (K_m and k_{cat}) were determined by nonlinear regression analysis of initial rates as a function of substrate concentration by using GraFit software (version 3.0; Erithacus Software Ltd., Staines, United Kingdom).

Kinetic parameters were also determined for the NS3–NS4A protein with the peptide substrate DDIVPC-SMSYTW-OH. Cleavage assays were performed at 23°C in the presence of 0.5 to 75 μM substrate, 1 nM biotin-DDIVPC-SMSY[^{125}I]TW-OH, and 2 to 15 nM NS3–NS4A protein in 50 mM Tris-HCl (pH 8.0)–0.25 M sodium citrate–0.01% *n*-dodecyl-β-D-maltoside–1 mM TCEP. The reaction was terminated by the sequential addition of 1 M morpholinoethanesulfonic acid (pH 5.8) and 0.5 N NaOH. The substrate was separated from the products by adding the assay mixture to avidin-coated agarose beads (Pierce), followed by a 60-min incubation at 23°C and filtration on a Millipore MADP N65 plate. The amount of radiolabeled product found in the filtrate was quantitated by using a Canberra-Packard TopCount detector or an LKB Multigamma detector. Kinetic parameter calculations were performed as described above.

***K_i* determination.** Protease activity was measured by continuous monitoring of the fluorescence change associated with cleavage of the fluorogenic depsipeptide substrates as described above. The initial velocity of the inhibited reaction was determined at several BILN 2061 concentrations (corresponding to a 25 to 75% inhibition range with the substrate at 2 K_m) while the substrate concentration was varied (typically from 0.5 to 5.0 K_m), assuming Michaelis-Menten kinetics. The reaction was initiated by enzyme addition. K_i calculations were performed by nonlinear regression analysis of the initial velocity data using the GraFit software. For the NS3 protease domains, some reported K_i values were calculated from the 50% inhibitory concentration (IC_{50}) based on the following equation for competitive inhibition: $IC_{50} = 0.5E_t + K_i\ (1 + S/K_m)$, where E_t is total enzyme concentration and S is substrate concentration. IC_{50}'s were obtained from the nonlinear curve fit the percent inhibition-concentration data of the Hill model applied to, by using SAS (Statistical Software System; SAS Institute Inc., Cary, N.C.).

RESULTS

Characterization of the NS3–NS4A proteases of genotypes 1, 2, and 3. A comparative analysis of protease activity was performed using the NS3–NS4A full-length proteins of HCV genotypes 1a, 1b, 2ac, 2b, and 3a. All NS3–NS4A proteins, when expressed in *E. coli*, autocleaved at the NS3/4A junction, resulting in a tight, stable heterodimeric complex that was purified via two chromatographic steps (data not shown). To facilitate comparisons between the different proteins, an internally quenched fluorogenic depsipeptide substrate and a peptide substrate, both derived from the genotype-1 NS5A/5B cleavage site, were used for all proteins. Alignment of the amino acids spanning the P6–P6′ region at the NS4A/4B, NS4B/5A, and NS5A/5B junctions revealed that the NS5A/5B sequence was the most conserved among genotypes.

Characterization of the various enzymes by use of the fluorogenic substrate (Table 1) showed similar catalytic efficiencies for genotypes 1, 2, and 3, ranging from 3.1×10^5 to 7.1×10^5 M^{-1} s^{-1}. The K_m and k_{cat} values differed less than threefold, ranging from 1.0 to 2.6 μM and 36 to 93 min^{-1}, respectively. Kinetic parameters determined in a radiometric assay using the peptide substrate also showed similar catalytic efficiencies, ranging from 3.2×10^4 to 6.9×10^4 M^{-1} s^{-1}. The K_m and k_{cat} values differed by less than six- and threefold, ranging from 1.9 to 12 μM and 7.2 to 23 min^{-1}, respectively. For all NS3–NS4A enzymes, however, the catalytic efficiencies obtained by using the fluorogenic depsipeptide substrate were approximately 10-fold higher than those obtained with the peptide substrate, mainly due to an increase in k_{cat}. For serine proteases, three steps are involved in substrate hydrolysis: substrate binding, acylation, and deacylation. The acyl enzyme is formed upon attack of the active-site serine on the carbonyl carbon of the substrate. Acylation is the rate-limiting step for amide substrates, while deacylation is rate-limiting for ester substrates. The similar values for k_{cat} with the ester substrate demonstrated that the enzymes of different genotypes exhibited no significant differences in deacylation rates. The similar k_{cat} values obtained with the peptide substrate also suggested similar acylation rates for all enzymes.

TABLE 1. Kinetic parameters of the NS3-NS4A heterodimer protein of genotypes 1, 2, and 3

Genotype	Kinetic parameters[a] for the following substrate:					
	Fluorogenic			Peptide		
	K_m (μM)	k_{cat} (min^{-1})	k_{cat}/K_m (M^{-1} s^{-1})	K_m (μM)	k_{cat} (min^{-1})	k_{cat}/K_m (M^{-1} s^{-1})
1a	2.6	48	3.1×10^5	5.4	13	4.0×10^4
1b	2.2	43	3.3×10^5	12	23	3.2×10^4
2ac	2.5	93	6.2×10^5	1.9	7.2	6.3×10^4
2b	2.1	90	7.1×10^5	2.1	7.5	6.0×10^4
3a	1.0	36	6.0×10^5	2.0	8.3	6.9×10^4

[a] Kinetic parameters were determined by using either the depsipeptide fluorogenic substrate anthranilyl-DDIVPAbu[C(O)-O]AMY(3-NO_2)TW-OH or the peptide substrate DDIVPC-SMSYTW-OH, as described in Materials and Methods. Data are averages from at least two separate determinations.

Inhibition of the NS3–NS4A proteases of genotypes 1, 2, and 3 with BILN 2061. The backbone amides of tripeptide NS3 protease inhibitors such as BILN 2061 (Fig. 1) are believed to interact with the active-site residues in the same way as do substrates. However, peptidic inhibitors derive their very high affinity for the active site in part by capitalizing on additional interactions. BILN 2061 was highly optimized for genotype-1

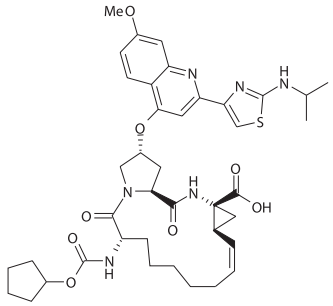

FIG. 1. Chemical structure of the macrocyclic inhibitor BILN 2061.

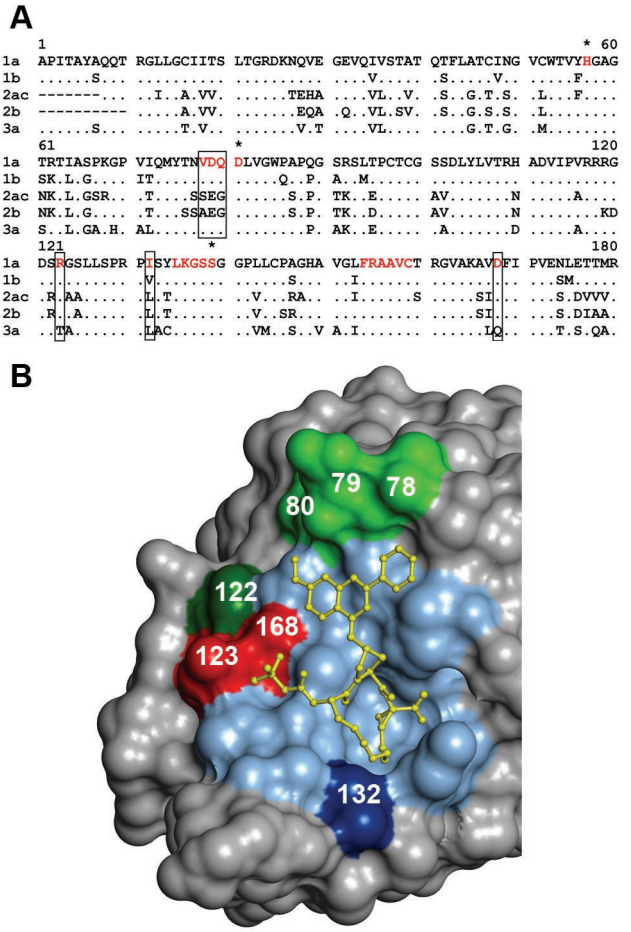

FIG. 2. Comparison of genotype-1a, -1b, -2b, -2ac, and -3a NS3 serine protease sequences. (A) Alignment of NS3 protease residues from genotypes 1a (NCBI accession no. AF009606), 1b, 2b, 2ac, and 3a (all obtained from HCV-infected individuals). Dots, residues in genotypes 1b, 2, and 3 that are identical to those in genotype 1a. Red letters, residues located within 5 Å of the inhibitor; those differing among genotypes are boxed. The catalytic triad residues are indicated by asterisks. (B) Structure of a macrocyclic tripeptide inhibitor bound to the active site of the NS3–NS4A$_{peptide}$ complex (genotype 1b) as determined by X-ray structure analysis (29). Residues located within 5 Å of the inhibitor are colored: light blue for residues conserved among genotypes, light green for residues differing between genotypes 1 and 2 (Val78, Asp79, Gln80), red for residues differing between genotypes 1 and 3 (Arg123, Asp168), and dark blue for Val132, which is replaced with a leucine in both genotypes 2 and 3. Dark green is used to identify Ser122, a residue located just outside of the 5-Å region that differs between genotypes 1 and 2.

enzymes; thus, binding of this inhibitor might be more sensitive to sequence differences than is substrate binding. We wished to determine how the affinity for BILN 2061 was affected by the sequence differences of enzymes from various genotypes (Fig. 2A). In vitro sensitivities of the NS3–NS4A proteins to BILN 2061 were evaluated, and K_i values are reported in Table 2. BILN 2061 is most active against genotypes 1a and 1b, with K_i values of 1.5 and 1.6 nM, respectively. These values are slightly higher than those previously reported with proteases expressed from recombinant baculoviruses (12). The genotype-2 and -3 proteins were less sensitive to inhibition by BILN 2061, with K_i values ranging from 83 to 90 nM, up to 56-fold higher than the K_i obtained for genotype 1b. The inhibition data indicate that binding of BILN 2061 is more sensitive to natural variation in the NS3–NS4A protease sequence than is binding of substrate peptides.

TABLE 2. NS3 protease inhibition with BILN 2061

Protease	K_i of BILN 2061[a] (nM) for genotype:				
	1a	1b	2ac	2b	3a
NS3–NS4A protein	1.5	1.6	86	83	90
NS3–NS4A$_{peptide}$	10	5.6	45	60	46
NS3	3.4[b]	44	525[b]	288[b]	230[b]

[a] Determined as described in Materials and Methods. Data are averages from at least two separate determinations.

[b] K_i calculated from the relationship between IC_{50} and K_i for competitive inhibition.

Role of inhibitor binding-site residues. We reasoned that variation of amino acids close to the bound inhibitor could account for the observed differences in sensitivity to BILN 2061. Nineteen residues located within 5 Å of the inhibitor were identified (Fig. 2A) by using the crystal structure of an inhibitor-enzyme complex previously reported for an analog of BILN 2061 (Fig. 2B) (29). This analog displayed affinities similar to those of BILN 2061 for the NS3–NS4A proteins of genotypes 1, 2, and 3 (unpublished data). Sequence alignment of the residues in the inhibitor binding site revealed that 13 out of these 19 residues were conserved. There are differences at positions 78 (Val, Ser, or Ala), 79 (Asp or Glu), 80 (Gln or Gly), 123 (Arg or Thr), 132 (Ile, Val, or Leu), and 168 (Asp or Gln) (Fig. 2). To determine the degree to which the decrease in the affinity of BILN 2061 toward genotype-2 and -3 proteases was attributable to differences in these inhibitor binding-site residues, NS3–NS4A mutant enzymes were constructed. The residues in genotype 1b were replaced with the corresponding binding-site residues for genotypes 2b and 3a, to yield chimeric enzymes designated 1b/2b$_{IBS}$ (V78A D79E Q80G V132L) and 1b/3a$_{IBS}$ (R123T V132L D168Q).

The activities of the genotype chimeras were assessed by using the peptide substrate DDIVPC-SMSYTW-OH. The K_m and k_{cat} values observed for both 1b/2b$_{IBS}$ and 1b/3a$_{IBS}$ were similar to those obtained with the parental 1b enzyme, although the differences in these parameters are relatively small among the various enzymes (Fig. 3A and B). However, the binding of the NS3 protease inhibitor BILN 2061 was significantly affected by the mutations. For the 1b/2b$_{IBS}$ mutant enzyme, a K_i of 13 nM was observed, in comparison to K_i's of 1.6 and 83 nM for the 1b and 2b enzymes, respectively (Fig. 3C), suggesting that the four mutated residues partially account for the loss of affinity for BILN 2061. Based on examination of the crystal structure, we postulated that serine 122, located in close proximity to the inhibitor binding site and replaced by an arginine in genotype 2, might also be involved in inhibitor binding (Fig. 2B). Introduction of the S122R mutation into the genotype 1b/2b$_{IBS}$ mutant enzyme had no effect on the kinetic parameters (Fig. 3A and B) but resulted in a threefold decrease in affinity for BILN 2061 (K_i, 38 nM) when compared to that of 1b/2b$_{IBS}$ (Fig. 3C). Overall, our data suggest that the

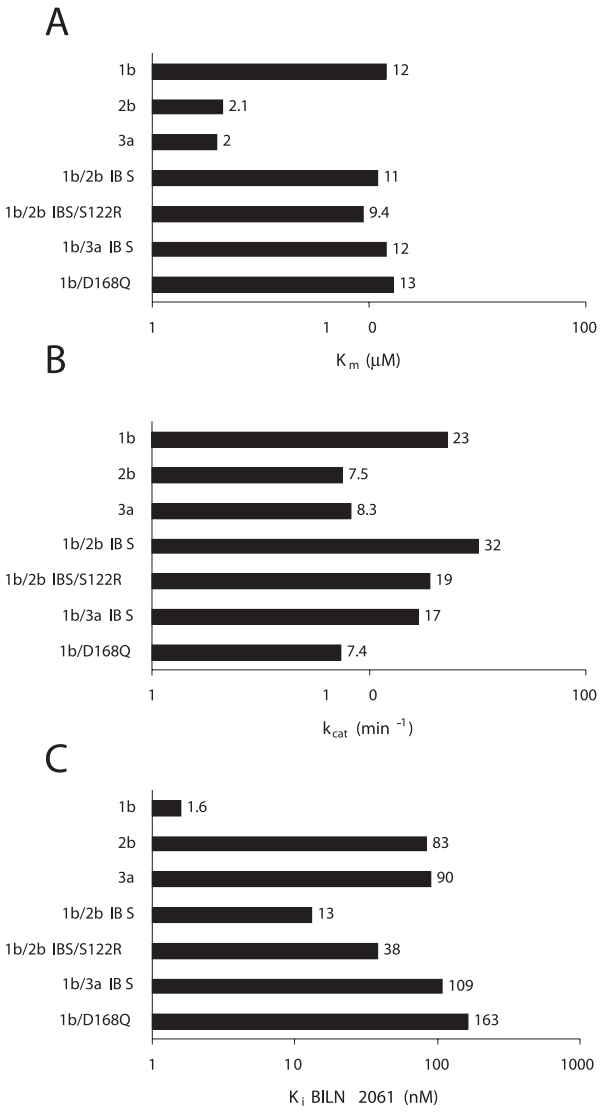

FIG. 3. Effects of mutations of inhibitor binding residues on NS3–NS4A protein protease activity and on BILN 2061 binding. The NS3–NS4A protein mutants 1b/2b$_{IBS}$ (V78A D79E Q80G V132L), 1b/2b$_{IBS}$/S122R, 1b/3a$_{IBS}$ (R123T V132L D168Q), and 1b/D168Q were compared to the NS3–NS4A proteins of genotypes 1b, 2b, and 3a with regard to K_m (A) and k_{cat} (B) values for the peptide substrate DDIVPC-SMSYTW-OH and K_i values for BILN 2061 (C). Kinetic parameters and inhibition constants were determined as described in Materials and Methods.

five mutated residues account for approximately 80% of the binding energy difference for BILN 2061.

The binding of BILN 2061 to the 1b/3a$_{IBS}$ enzyme (K_i, 109 nM) was similar to its binding to the 3a protein (K_i, 90 nM) (Fig. 3C), suggesting that 3a residues Thr123, Leu132, and Gln168 account for the increase in K_i observed with the genotype-3a enzyme. The D168Q single-substitution mutant was also generated, since resistance studies recently conducted with an analog of BILN 2061 identified position 168 as being responsible for the resistance phenotype (28). The D168Q mutation, when compared to the wild type, did not affect substrate binding (Fig. 3A) but resulted in a reduction in k_{cat} similar to that observed for the 3a protein (Fig. 3B). A K_i of 163 nM, slightly higher than that observed for 1b/3a$_{IBS}$, was obtained for the single-amino-acid substitution (Fig. 3C). The data for the D168Q mutant confirmed its significant role in BILN 2061 binding but further suggested that other differences at position 123 and/or 132 mitigate the effect of the D168Q substitution on sensitivity to BILN 2061.

TABLE 3. Kinetic parameters of the NS3-NS4A$_{peptide}$ complex and of the NS3 protease domain of genotypes 1, 2, and 3[a]

Genotype	Protease					
	NS3pr-NS4A$_{peptide}$			NS3pr		
	K_m (μM)	k_{cat} (min^{-1})	k_{cat}/K_m (10^4 M^{-1} s^{-1})	K_m (μM)	k_{cat} (min^{-1})	k_{cat}/K_m (10^4 M^{-1} s^{-1})
1a	11	11	1.7	0.20	2.2	18
1b	7.1	20	4.7	0.34	1.5	7.4
2ac	5.5	6.2	1.9	0.55	2.0	6.1
2b	5.7	9.7	2.8	0.69	2.1	5.1
3a	1.6	12	12	0.21	0.51	4.0

[a] Kinetic parameters were determined by using the depsipeptide fluorogenic substrate anthranilyl-DDIVPAbu[C(O)-O]AMY(3-NO_2)TW-OH, as described in Materials and Methods. Data are averages from at least two separate determinations.

Characterization of the NS3 protease domains of genotypes 1, 2, and 3. NS3 protease domains were characterized in the presence and absence of NS4A cofactor peptides in order to help assess the contributions of the C-terminal helicase domain of NS3 as well as the NS4A cofactor to catalytic activity and inhibitor binding. NS4A increases the protease activity of NS3 and is required to achieve optimal conformation of the NS3 protease active site (9, 33). Since the central hydrophobic domain is sufficient for cofactor activity (14), we evaluated the activity of each NS3 protease domain in the presence of this truncated NS4A, using the fluorogenic depsipeptide substrate and an assay buffer containing 30% glycerol to favor complex formation. For each NS3 protease domain, specific cofactor peptides were synthesized with the sequence of the central domain of the corresponding NS4A protein. A 1,000-fold molar excess was added relative to the protease concentration. Similar kinetic parameters were observed for the NS3 protease–NS4A$_{peptide}$ complexes, with at most a sevenfold difference in k_{cat}/K_m (Table 3). K_m values ranged from 1.6 to 11 μM, and k_{cat} values ranged from 6.2 to 20 min^{-1}. The activities of the NS3 protease–NS4A$_{peptide}$ complexes and the NS3–NS4A proteins were measured under their respective optimal physicochemical conditions for enzymatic catalysis. Comparison of the catalytic efficiencies for all NS3 protease–NS4A$_{peptide}$ complexes, ranging from 1.7×10^4 to 12×10^4 M^{-1} s^{-1}, to the values obtained for the corresponding NS3–NS4A proteins revealed 5- to 33-fold-lower values for the complexes (Table 1). This finding might suggest the requirement of the helicase domain and/or the full-length NS4A cofactor for optimal activity of the protease, but it could be due in part to differences in assay buffers required for optimal activity of each protease form. In vitro sensitivities of the NS3 protease–NS4A$_{peptide}$ complexes to BILN 2061 were also evaluated, and K_i values are reported in Table 2. As observed with the NS3–NS4A protein, BILN 2061 is most active against genotypes 1a (K_i, 10 nM) and

1b (K_i, 5.6 nM); the genotype-2 and -3 enzymes are less sensitive to inhibition by BILN 2061, with K_i values (45 to 60 nM) 4.5- to 11-fold higher than those obtained for genotype 1b. Whereas for the genotype-1 enzymes the full-length protein exhibited a slightly higher affinity for BILN 2061 than did the protease domain-peptide complex, the difference in affinity was less pronounced for genotypes 2 and 3. These results indicate that, at least for these genotypes, residues of the helicase domain and of the full-length NS4A protein do not appear to significantly contribute to or interfere with inhibitor binding.

In the absence of the $NS4A_{peptide}$, the catalytic efficiencies (k_{cat}/K_m) of the NS3 protease domains (Table 3) differed less than fivefold and, with the exception of genotype 3a, were slightly higher than the values obtained for the NS3 protease–$NS4A_{peptide}$ complexes. However, relative to values for the NS3 protease–$NS4A_{peptide}$ complexes, lower K_m values (up to a 55-fold decrease), ranging from 0.20 to 0.69 μM, and lower k_{cat} values (up to a 24-fold decrease), ranging from 0.51 to 2.2 min^{-1}, were observed. The low K_m for the NS5A/5B fluorogenic substrate probably accounts for the comparable catalytic efficiencies observed in the presence of the $NS4A_{peptide}$. By use of the previously described NS4A/4B-derived depsipeptide fluorogenic substrate, for which higher K_m values were reported for the protease domain (27), an increase in protease activity was observed in the presence of the NS4A cofactor for all of the genotypes evaluated, and similar catalytic efficiencies were found for the different genotypes (data not shown). As expected, BILN 2061 is again most active against genotypes 1a and 1b (Table 2). However, the K_i for the 1a protease was reproducibly lower in the absence of the $NS4A_{peptide}$ than in its presence (3.4 versus 10 nM, respectively). For genotype-2 and -3 enzymes, K_i values ranged from 230 to 525 nM, 5- to 12-fold higher than those obtained for the 1b protease domain.

DISCUSSION

The NS3 protease inhibitor BILN 2061 has been shown to rapidly reduce viral RNA plasma levels in patients infected with genotype-1 HCV. The drug discovery effort which led to this inhibitor was targeted toward genotype-1 virus because of the significant unmet medical need in this infected population. However, other HCV genotypes, in particular genotypes 2 and 3, also account for a large proportion of infections worldwide. In this study, we have compared the kinetic profiles of NS3 proteases from genotypes 1, 2, and 3 and their sensitivities to BILN 2061. The similarity of these kinetic profiles within each protease form studied supports the expectation that the overall conformation of the substrate binding site is conserved among the natural HCV variants, since substrate recognition for the NS3 protease relies on multiple weak interactions extended over several peptide bonds (10). Differences among genotypes in amino acids located in the substrate binding site have only a weak effect on substrate recognition and protease activity for the three enzyme forms used.

Our results are consistent with those of a previous study in which the activity of a single-chain $NS4A_{peptide}$–NS3 protease of genotypes 1a, 1b, and 3a was evaluated by using peptide substrates corresponding to the NS4A/4B, NS4B/5A, and NS5A/5B cleavage sites of genotype 1 or 3a (1). However, the similarity in genotype-1, -2, and -3 protease activities was observed with short, unnatural cleavage junction substrates. Examination of processing using in vitro-translated NS4A/4B, NS4B/5A, and NS5A/5B polyprotein fragments from genotype 1a revealed no measurable differences in protease activities for genotype-1 and -3 single-chain $NS4A_{peptide}$–NS3 proteases (1) but a reduction in activity for the genotype-2 NS3 protease–$NS4A_{peptide}$ complex relative to that of genotypes 1 and 3 (32). Additional studies with polyprotein substrates are therefore required.

The in vitro inhibition studies conducted with all three protease forms showed that BILN 2061 is more active against genotypes 1a and 1b than against non-1 genotypes, although the fold increase in K_i for genotypes 2 and 3 varies with the protease form. We observed increases in K_i with the genotype-2 and -3 proteases ranging from 52- to 60-fold, 4- to 11-fold, and 5- to 12-fold for the NS3–NS4A protein, the NS3 protease–$NS4A_{peptide}$ complex, and the NS3 protease, respectively, over values obtained with the genotype-1a or -1b enzymes. Such an observation was expected, since our NS3 protease inhibitor series was optimized for genotype-1 enzymes. However, the residues that are in direct contact with the inhibitor, as determined by X-ray data of an inhibitor-enzyme complex, are well conserved, predicting that this class of inhibitor would be active against all genotypes and subtypes. These differences in affinity among genotypes were observed using in vitro conditions optimized for enzymatic activity and more specifically for the genotype-1 enzymes. Comparison of the activity of inhibitors against the different genotypes in an HCV viral replication system or the surrogate HCV RNA replicon model will more accurately reflect their efficacy in patients infected with the different viral strains. Such comparisons should be carried out as soon as non-genotype-1 replication systems become available. Altogether, the observed kinetic profiles and the inhibitor sensitivity studies with the enzymes of various genotypes suggest that the interaction of BILN 2061 with NS3 is more sensitive to the naturally occurring polymorphism of the protease than are peptide substrates. This is, in part, due to the increased conformational rigidity of this class of inhibitors (29) as well as to distinct interactions, including a reduction in hydrogen bonding but additional hydrophobic interactions.

In some cases, amino acid differences distant from the binding site have been reported to affect inhibitor affinity (19), but we found that substitutions close to the inhibitor binding site explained most of the differences observed for BILN 2061. Chimeric NS3–NS4A proteins were made in which residues of the 1b protein close to the inhibitor binding site of the enzyme were substituted for their non-genotype-1 equivalents. Substitutions made for the first $1b/2b_{IBS}$ chimera, a cluster of residues at amino acids 78 to 80 as well as residue 132, accounted for approximately one-half of the binding-energy difference between the genotype-1 and -2 enzymes. This is most likely due to residues 78 to 80, located on the E1–F1 loop, which is in close proximity to the quinoline moiety of the inhibitor. We also determined that residue 122, in which the serine found in genotype 1 was replaced with arginine, also plays a role in inhibitor binding. Residue 122 is close to charged residues Asp168 and Arg123, and replacement of the neutral serine by arginine could alter the hydrogen-bonding pattern in this region, thus affecting inhibitor binding, as has been discussed for

substitutions at position 168 (28) (see also below). Additional mutagenesis studies will be required to identify other residue differences which have an impact on inhibitor binding.

The genotype-3a protein and the 1b/3a$_{IBS}$ chimera were found to have similar sensitivities to BILN 2061. Furthermore, the genotype-3 residue Gln168 was identified as the major determinant for the loss of affinity of this inhibitor for the genotype-3a protease. This observation is consistent with the crystal structure of an analog of BILN 2061 bound to the NS3 protease–NS4A$_{peptide}$ complex, which revealed that the P2 group of the inhibitor facilitated the formation of a salt bridge between Arg155 and Asp168 (29). This could explain how mutation of Asp168 would have a significant effect on inhibitor binding even though this residue is not in direct contact with the inhibitor. The 1b/3a$_{IBS}$ chimera in which both amino acids 123 and 168 were mutated to polar but neutral threonine and glutamine had a slightly higher affinity for the inhibitor than did the D168Q enzyme. Mutation of both residues together preserves the net charge and may result in a less significant change in the conformation or solvation of Arg155 and, consequently, in a less significant change in the binding of BILN 2061. Amino acid 168 was previously identified in a resistance study using an acyclic analog of BILN 2061 (28). Interestingly, the substitutions D168V and D168Y found in this study had a larger effect on BILN 2061 binding than the substitution with glutamine (data not shown). An earlier study comparing genotype-1b and -3a proteases had also evaluated the contribution of residues 123 and 168 to the binding of less-optimized hexapeptide-like inhibitors (1). The residue at position 123 alone quantitatively accounted for the differences in sensitivities between genotype-1 and -3a enzymes, while substitution of residue 168 alone had no effect on inhibitor binding in this case. The latter result reflects the differences between the interactions of these two classes of inhibitors with the protease active site.

The residue at position 132 is also different in different genotypes and subtypes, but substitutions are conservative. Residue 132 is a member of the S1–S3 pocket and has been suggested to interact with the aliphatic macrocycle ring of the inhibitor (29). Since genotype-1a and -1b enzymes have similar affinities for BILN 2061, we believe that these conservative substitutions at position 132 are likely to have a modest role in the binding of BILN 2061.

Administration of 25 to 500 mg of BILN 2061 twice daily to genotype-1 HCV-infected patients for 2 days resulted in a 2- to 3-log$_{10}$-unit reduction in HCV RNA plasma levels for all patients treated [Hinrichsen et al., Hepatology **36**(Suppl. 1)**:**297A, 2002]. The low-nanomolar K_i values reported here suggest that BILN 2061 should be effective in the treatment of patients with genotype-2 and -3 infections. In fact, a recently reported trial in which 500 mg of BILN 2061 was administered twice daily for 2 days to patients infected with non-genotype-1 viruses indicated a significant reduction in HCV RNA plasma levels for the majority of patients, although the response was not as robust as that observed for genotype-1 infections (M. Reiser, H. Hinrichsen, Y. Benhamou, R. Sentjens, H. Wedemeyer, L. Calleja, X. Forns, J. Croenlein, C. Yong, G. Nehmiz, and G. Steinmann, abstract from the 54th Ann. Meet. Am. Assoc. Study Liver Dis., 2003, Hepatology **38**(Suppl. 1)**:**221A, 2003; also unpublished data). Interestingly, the NS3 proteases of genotypes 2 and 3 used in this study were derived from patients exhibiting a broad range of viral-load reductions upon BILN 2061 administration. We found that the response observed for the source patient was not dependent on the in vitro sensitivity to BILN 2061. The less-robust in vivo efficacy of BILN 2061 for patients with genotype-2 and -3 infections may depend not only on the reduced in vitro inhibitory activity but also on differences in the replication kinetics for different genotypes and patient-to-patient differences in viral replication and compound pharmacokinetic properties. In particular, variation in viral kinetics has been identified as a major determinant in disease progression (7). The use of a specific anti-HCV agent such as BILN 2061 should allow a better estimation of the viral-replication kinetics in infected patients than those obtained with the less-specific treatment of interferon plus ribavirin.

ACKNOWLEDGMENTS

We thank Dominik Wernic for NS4A peptide and substrate synthesis; Vida Gorys for BILN 2061 synthesis; Mireille Cartier for sequence alignments; Lynn Amon for molecular modeling; Nathalie Goudreau for providing Fig. 2B; Amélie Fradet-Turcotte, Yelena Markovich, and Joseph Walton for valuable technical assistance; and Montse Llinás-Brunet for critical reading of the manuscript. Finally, we are grateful to Michael G. Cordingley for his continuous support.

REFERENCES

1. **Beyer, B. M., R. Zhang, Z. Hong, V. Madison, and B. A. Malcolm.** 2001. Effect of naturally occurring active site mutations on hepatitis C virus NS3 protease specificity. Proteins **43:**82–88.
2. **Bianchi, E., C. Steinkühler, M. Taliani, A. Urbani, R. De Francesco, and A. Pessi.** 1996. Synthetic depsipeptide substrates for the assay of human hepatitis C virus protease. Anal. Biochem. **237:**239–244.
3. **Bodansky, M.** 1993. Peptide chemistry, 2nd ed. Springer-Verlag, Berlin, Germany.
4. **Di Bisceglie, A. M., and J. H. Hoofnagle.** 2002. Optimal therapy of hepatitis C. Hepatology **36:**S121–S127.
5. **Domingo, E., C. M. Ruiz-Jarabo, S. Sierra, A. Arias, N. Pariente, E. Baranowski, and C. Escarmís.** 2002. Emergence and selection of RNA virus variants: memory and extinction. Virus Res. **82:**39–44.
6. **Drake, J. W., and J. J. Holland.** 1999. Mutation rates among RNA viruses. Proc. Natl. Acad. Sci. USA **96:**13910–13913.
7. **Hoofnagle, J. H.** 2002. Course and outcome of hepatitis C. Hepatology **36:**S21–S29.
8. **Kakiuchi, N., M. Hijikata, Y. Komoda, Y. Tanji, Y. Hirowatari, and K. Shimotohno.** 1995. Bacterial expression and analysis of cleavage activity of HCV serine proteinase using recombinant and synthetic substrate. Biochem. Biophys. Res. Commun. **210:**1059–1065.
9. **Kim, J. L., K. A. Morgenstern, C. Lin, T. Fox, M. D. Dwyer, J. A. Landro, S. P. Chambers, W. Markland, C. A. Lepre, E. T. O'Malley, S. L. Harbeson, C. M. Rice, M. A. Murcko, P. R. Caron, and J. A. Thomson.** 1996. Crystal structure of the hepatitis C virus NS3 protease domain complexed with a synthetic NS4A cofactor peptide. Cell **87:**343–355.
10. **Koch, U., G. Biasiol, M. Brunetti, D. Fattori, M. Pallaoro, and C. Steinkühler.** 2001. Role of charged residues in the catalytic mechanism of hepatitis C virus NS3 protease: electrostatic precollision guidance and transition-state stabilization. Biochemistry **40:**631–640.
11. **Kolykhalov, A. A., K. Mihalik, S. M. Feinstone, and C. M. Rice.** 2000. Hepatitis C virus-encoded enzymatic activities and conserved RNA elements in the 3′ nontranslated region are essential for virus replication in vivo. J. Virol. **74:**2046–2051.
12. **Lamarre, D., P. C. Anderson, M. Bailey, P. Beaulieu, G. Bolger, P. Bonneau, M. Bös, D. R. Cameron, M. Cartier, M. G. Cordingley, A.-M. Faucher, N. Goudreau, S. Kawai, G. Kukolj, L. Lagacé, S. R. LaPlante, H. Narjes, M.-A. Poupart, J. Rancourt, R. E. Sentjens, R. St. George, B. Simoneau, G. Steinmann, D. Thibeault, Y. S. Tsantrizos, S. M. Weldon, C.-L. Yong, and M. Llinàs-Brunet.** 2003. An NS3 protease inhibitor with antiviral proof-of-concept in humans infected with hepatitis C virus. Nature **426:**186–189.
13. **LaPlante, S. R., D. R. Cameron, N. Aubry, S. Lefebvre, G. Kukolj, R. Maurice, D. Thibeault, D. Lamarre, and M. Llinàs-Brunet.** 1999. Solution structure of substrate-based ligands when bound to hepatitis C virus NS3 protease domain. J. Biol. Chem. **274:**18618–18624.
14. **Lin, C., J. A. Thomson, and C. M. Rice.** 1995. A central region in the

hepatitis C virus NS4A protein allows formation of an active NS3–NS4A serine proteinase complex in vivo and in vitro. J. Virol. **69:**4373–4380.

15. **Llinàs-Brunet, M., M. Bailey, R. Déziel, G. Fazal, V. Gorys, S. Goulet, T. Halmos, R. Maurice, M. Poirier, M.-A. Poupart, J. Rancourt, D. Thibeault, D. Wernic, and D. Lamarre.** 1998. Studies on the C-terminal of hexapeptide inhibitors of the hepatitis C virus serine protease. Bioorg. Med. Chem. Lett. **8:**2719–2724.
16. **Llinàs-Brunet, M., M. Bailey, G. Fazal, E. Ghiro, V. Gorys, S. Goulet, T. Halmos, R. Maurice, M. Poirier, M.-A. Poupart, J. Rancourt, D. Thibeault, D. Wernic, and D. Lamarre.** 2000. Highly potent and selective peptide-based inhibitors of the hepatitis C virus serine protease: towards smaller inhibitors. Bioorg. Med. Chem. Lett. **10:**2267–2270.
17. **Llinàs-Brunet, M., M. Bailey, G. Fazal, S. Goulet, T. Halmos, S. R. LaPlante, R. Maurice, M. Poirier, M.-A. Poupart, D. Thibeault, D. Wernic, and D. Lamarre.** 1998. Peptide-based inhibitors of the hepatitis C virus serine protease. Bioorg. Med. Chem. Lett. **8:**1713–1718.
18. **Mondelli, M. U., and E. Silini.** 1999. Clinical significance of hepatitis C virus genotypes. J. Hepatol. **31**(Suppl. 1)**:**65–70.
19. **Muzammil, S., P. Ross, and E. Freire.** 2003. A major role for a set of non-active site mutations in the development of HIV-1 protease drug resistance. Biochemistry **42:**631–638.
20. **Neumann, A. U., N. P. Lam, H. Dahari, D. R. Gretch, T. E. Wiley, T. J. Laydent, and A. S. Perelson.** 1998. Hepatitis C viral dynamics in vivo and the antiviral efficacy of interferon-alpha therapy. Science **282:**103–107.
21. **Pause, A., G. Kukolj, M. Bailey, M. Brault, F. Dô, T. Halmos, L. Lagacé, R. Maurice, M. Marquis, G. McKercher, C. Pellerin, L. Pilote, D. Thibeault, and D. Lamarre.** 2003. An NS3 serine protease inhibitor abrogates replication of subgenomic hepatitis C virus RNA. J. Biol. Chem. **278:**20374–20380.
22. **Pawlotsky, J.-M.** 2003. Hepatitis C virus genetic variability: pathogenic and clinical implications. Clin. Liver Dis. **7:**45–66.
23. **Reed, K. E., and C. M. Rice.** 2000. Overview of hepatitis C virus genome structure, polyprotein processing, and protein properties. Curr. Top. Microbiol. Immunol. **242:**55–84.
24. **Simmonds, P.** 1999. Viral heterogeneity of the hepatitis C virus. J. Hepatol. **31**(Suppl. 1)**:**54–60.
25. **Simmonds, P.** 2001. The origin and evolution of hepatitis viruses in humans. J. Gen. Virol. **82:**693–712.
26. **Steinhühler, C., U. Koch, F. Narjes, and V. G. Matassa.** 2001. Hepatitis C virus serine protease inhibitors: current progress and future challenges. Curr. Med. Chem. **8:**919–932.
27. **Taliani, M., E. Bianchi, F. Narjes, M. Fossatelli, A. Urbani, C. Steinkühler, R. De Francesco, and A. Pessi.** 1996. A continuous assay of hepatitis C virus protease based on resonance energy transfer depsipeptide substrates. Anal. Biochem. **240:**60–67.
28. **Trozzi, C., L. Bartholomew, A. Ceccacci, G. Biasiol, L. Pacini, S. Altamura, F. Narjes, E. Muraglia, G. Paonessa, U. Koch, R. De Francesco, C. Steinkühler, and G. Migliaccio.** 2003. In vitro selection and characterization of hepatitis C virus serine protease variants resistant to an active-site peptide inhibitor. J. Virol. **77:**3669–3779.
29. **Tsantrizos, Y. S., G. Bolger, P. Bonneau, D. R. Cameron, N. Goudreau, G. Kukolj, S. R. LaPlante, M. Llinàs-Brunet, H. Nar, and D. Lamarre.** 2003. Macrocyclic inhibitors of the NS3 protease as potential therapeutic agents of hepatitis C virus infection. Angew. Chem. Int. Ed. **42:**1355–1360.
30. **Tsantrizos, Y. S., D. R. Cameron, A.-M. Faucher, É. Ghiro, N. Goudreau, T. Halmos, and M. Llinàs-Brunet.** August 2003. Macrocyclic peptides active against hepatitis C virus. U.S. patent 6,608,027 B1.
31. **Webster, G., E. Barnes, D. Brown, and G. Dusheiko.** 2000. HCV genotypes—role in pathogenesis of disease and response to therapy. Baillière's Clin. Gastroenterol. **14:**229–240.
32. **Wright-Minogue, J., N. Yao, R. Zhang, N. Butkiewicz, B. M. Baroudy, J. Y. N. Lau, and Z. Hong.** 2000. Cross-genotypic interaction between hepatitis C virus NS3 protease domains and NS4A cofactors. J. Hepatol. **32:** 497–504.
33. **Yan, Y., Y. Li, S. Munshi, V. Sardana, J. L. Cole, M. Sardana, C. Steinkühler, L. Tomei, R. De Francesco, L. C. Kuo, and Z. Chen.** 1998. Complex of NS3 protease and NS4A peptide of BK strain hepatitis C virus: a 2.2 Å resolution structure in a hexagonal crystal form. Protein Sci. **7:**837–847.